Cooperative enhancement of the nonlinear optical response in conjugated energetic materials: A TD-DFT study

Andrew E. Sifain,[1,2] Loza F. Tadesse,[3] Josiah A. Bjorgaard,[2,4] David E. Chavez,[5] Oleg V. Prezhdo,[1,6] R. Jason Scharff,[5,a)] and Sergei Tretiak[2,4,7,b)]
[1]*Department of Physics and Astronomy, University of Southern California, Los Angeles, California 90089-0485, USA*
[2]*Center for Nonlinear Studies, Los Alamos National Laboratory, Los Alamos, New Mexico 87545, USA*
[3]*Department of Bioengineering, Stanford University, Stanford, California 94305-4125, USA*
[4]*Theoretical Division, Los Alamos National Laboratory, Los Alamos, New Mexico 87545, USA*
[5]*Explosives Science and Shock Physics Division, Los Alamos National Laboratory, Los Alamos, New Mexico 87545, USA*
[6]*Department of Chemistry, University of Southern California, Los Angeles, California 90089-1062, USA*
[7]*Center for Integrated Nanotechnologies, Los Alamos National Laboratory, Los Alamos, New Mexico 87545, USA*

(Received 13 December 2016; accepted 28 February 2017; published online 21 March 2017)

Conjugated energetic molecules (CEMs) are a class of explosives with high nitrogen content that posses both enhanced safety and energetic performance properties and are ideal for direct optical initiation. As isolated molecules, they absorb within the range of conventional lasers. Crystalline CEMs are used in practice, however, and their properties can differ due to intermolecular interaction. Herein, time-dependent density functional theory was used to investigate one-photon absorption (OPA) and two-photon absorption (TPA) of monomers and dimers obtained from experimentally determined crystal structures of CEMs. OPA scales linearly with the number of chromophore units, while TPA scales nonlinearly, where a more than 3-fold enhancement in peak intensity, per chromophore unit, is calculated. Cooperative enhancement depends on electronic delocalization spanning both chromophore units. An increase in sensitivity to nonlinear laser initiation makes these materials suitable for practical use. This is the first study predicting a cooperative enhancement of the nonlinear optical response in energetic materials composed of relatively small molecules. The proposed model quantum chemistry is validated by comparison to crystal structure geometries and the optical absorption of these materials dissolved in solution. *Published by AIP Publishing.* [http://dx.doi.org/10.1063/1.4978579]

I. INTRODUCTION

There has been an increasing effort to design energetic materials that are safe and easy to handle. While the motivation to do so is obvious, it is rather difficult in practice, as it requires decoupling the correlation between explosive performance and sensitivity.[1–8] Current methods used to detonate high explosives are electrical or mechanical.[9] These methods are not inherently safe, however, because coincidental electrical or mechanical insults can result in unwarranted detonation. Recent efforts have focused on photoactive energetic materials with absorption within the range of conventional lasers.[10–23] Introducing a fiber optic cable for direct optical initiation eliminates sensitivity to electrical insults, while replacing primary explosives with less sensitive secondary explosives reduces sensitivity to mechanical insults. A class of energetic materials that exhibit the optical, electrical, and mechanical properties suitable for this application are conjugated energetic molecules (CEMs).

CEMs are secondary explosives with a large number of N–N and C–N bonds, which raise their heat of formation.[3–6,24–33] Moreover, their planar, conjugated structure with electronic delocalization increases density and molecular stability. Their synthetic versatility has been evidenced in nitrogen-rich heterocycles such as triazole, tetrazole, and tetrazine.[30] A recent theoretical work has highlighted structure-property relationships, such as adding oxygen to the core framework to simultaneously increase the two-photon absorption (TPA) cross section and increase oxygen balance;[21] a measure of the oxygen to fuel ratio that determines explosive strength.[34] While past works have discussed isolated CEMs, more work is needed to characterize their associated crystal structures used in practice.

The synthesis and characterization of crystalline CEMs have been recently reported.[35–40] These materials are generally less sensitive to electrical and mechanical stimuli than traditional explosives such as pentaerythritol tetranitrate (PETN), 1,3,5-trinitroperhydro-1,3,5-triazine (RDX), and octahydro-1,3,5,7-tetranitro-1,3,5,7-tetrazocine (HMX), while maintaining strong explosive performance. However, the optical properties of these materials have not yet been determined, as direct evaluation via optical detonation experiments can often be difficult and costly. It is beneficial to have a qualitative and quantitative overview of the optical performance *a priori*, which can be accomplished using modern computational techniques for predictive modeling. The majority of CEMs from our last study were optically excited within the range of

a)Electronic mail: scharff@lanl.gov
b)Electronic mail: serg@lanl.gov

500–250 nm (2.5–5.0 eV).[21] However, due to the availability of high power Nd:YAG lasers, the most practical wavelength for initiation is 1064 nm (≈1.2 eV). One possible avenue for optical excitation is by degenerate TPA, whereby a material simultaneously absorbs two photons of the same energy. Increasing the sensitivity of these materials to nonlinear laser initiation eliminates the need of electrical and mechanical stimuli for detonation. One such mechanism for increasing TPA intensity is cooperative enhancement.

Cooperative enhancement of TPA is due to the interaction between multiple chromophore units and is observed when the maximum TPA cross section, per chromophore unit, is considerably larger than that of an individual, noninteracting unit. It is attributed to π-conjugation, where the delocalization of a coherent electronic molecular wavefunction spans multiple building blocks of the compound, which increases transition dipole moments. Strong cooperative enhancements have been measured in dendrimers,[41–45] substituted porphyrins,[46] porphyrin dimers,[47,48] linear porphyrin[49] and squaraine oligomers,[50] multichromophoric compounds,[51] and self-assembled zinc-porphyrin nanostructures.[52] By utilizing time-dependent density functional theory (TD-DFT), we calculate a cooperative enhancement in dimers extracted from crystalline CEMs, thereby providing the first evidence of a strong nonlinear optical response in energetic materials composed of relatively small molecules for explosive applications.

II. CONJUGATED ENERGETIC MATERIALS

This section provides readers with a concise overview of recent measurements and theoretical predictions covering both the safety as well as energetic performance properties of the materials studied in this paper. It is worth noting that these data are those of the bulk materials, whereas the focus of this paper is on the optical properties of monomers and dimers extracted from their corresponding crystal structures. However, we find it useful to not only motivate these materials as they are used in practice but to also present data from several works in a single location for comparison.

We study molecular materials **A** through **C**, which comprise the corresponding CEMs shown in Fig. 1. Molecule **A** has a tetrazine-tetrazolo bicyclic framework with two oxygen substituents and a NH_2 substituent. Molecule **B** has a triazine-triazolo bicyclic framework with two NO_2 substituents and a NH_2 substituent. Molecule **C** has a single cyclic tetrazine system with two fluorinated chain-like substituents and two oxygen substituents. The synthesis and characterization of their corresponding crystal structures are provided in Refs. 35 and 36 for **A**, Refs. 37 and 38 for **B**, and Refs. 39 and 40 for **C**. Table I shows sensitivity data of these materials, as well as those of conventional explosive materials. Data for PETN and RDX were taken from Refs. 35 and 36. *Impact* is the minimum energy at which a falling weight causes an explosive material under total confinement to initiate. *Spark*, also known as electrostatic discharge (ESD), is the minimum electrostatic energy discharged from a capacitor to an explosive material at which initiation occurs. Last, *friction* determines whether or not an explosive material is susceptible to initiation by a specified frictional force. The details of the experiments carried out to obtain these results can be found in the references above.

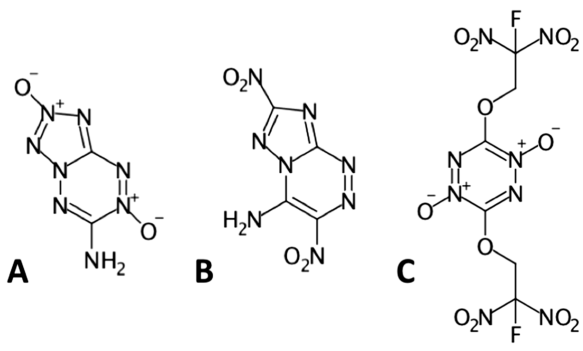

FIG. 1. Chemical structures of the CEMs.

As shown in Table I, these materials show excellent insensitivities toward destructive electrical and mechanical stimuli. Material **B** was found to be relatively insensitive to impact, spark, and friction. Material **A**, although more sensitive than **B**, was found to be less sensitive than PETN and RDX overall. The insensitivities of **C** are similar to those of **A**. Materials **A** through **C** were also found to have good thermal stabilities, with decomposition occurring above 150 °C for **A**, 232 °C for **B**, and 174 °C for **C**. PETN and RDX decompose above 164 °C[53] and 210 °C,[54,55] respectively.

As a measure of explosive performance, we can compare theoretical predictions of the detonation pressure, p_D, and velocity, v_D, which are defined as the pressure and velocity of a shock wave front traveling through a detonated explosive. Theoretical predictions were calculated with the Cheetah thermochemical code.[56] Densities were measured at 293 K, while heats of formation were calculated with the methods described in Refs. 57 and 58 for **A** and **B** and Refs. 59 and 60 for **C**. Densities and heats of formations were fed into the Cheetah program to obtain p_D and v_D. These values are predicted to be 41.3 GPa and 9.6 km s^{-1} at 1.93 g cm^{-3} for **A**, 32.0 GPa and 8.7 km s^{-1} at 1.86 g cm^{-3} for **B**, and 40.6 GPa and 8.8 km s^{-1} at 1.96 g cm^{-3} for **C**. For PETN, these values are 33.2 GPa and 8.3 km s^{-1} at 1.77 g cm^{-3},[53] while for RDX, they are 34.9 GPa and 8.8 km s^{-1} at 1.80 g cm^{-3}.[54,55] Therefore, materials **A** through **C** are predicted to have higher detonation pressures and velocities than those of PETN and RDX, and with higher densities, which may imply more explosive power per unit volume. The details of the simulations carried out to obtain these results can be found in the aforementioned references.

Another factor of explosive performance is the oxygen balance (OB%), which provides a measure to which a material can be oxidized. On average, optimal explosive performance is

TABLE I. Sensitivity data of materials **A** through **C**, PETN, and RDX.

Structure	Impact (J)	Spark (J)	Friction (N)
A	6.0	0.062	109
B	29	0.125	360
C	5.6	0.062	104
PETN	2.5	0.062	92
RDX	6.0	0.062	87

achieved as OB% approaches zero.[61] The following equation was used to compute OB%,

$$\mathrm{OB\%} = -\frac{1600}{M}\left(2X + \frac{1}{2}Y - Z\right), \tag{1}$$

where X, Y, and Z, are the number of carbon, hydrogen, and oxygen atoms, respectively, and M is the molecular weight of the compound. The OB% of materials **A** through **C** are −28.0%, −35.4%, and −3.8%, respectively. The OB% of **C** was obtained by combining each fluorine to hydrogen to make hydrogen fluoride (HF), which were not included in the calculation for oxidation. For PETN ($C_5H_8N_4O_{12}$) and RDX ($C_3H_6N_6O_6$), these values are −10.1% and −22.6%, respectively. Overall, **A** through **C** show enhanced safety properties and promising energetic performance properties compared to conventional explosive materials. By determining their optical properties, we can assess their viability toward optical initiation.

III. COMPUTATIONAL METHODS

A. Optical absorption spectra

The one-photon absorption (OPA) of the monomers and dimers were calculated. The ground-state geometry of each monomer was extracted from a single molecule of its experimental crystal structure. A similar procedure was carried out to obtain the geometries of the dimers, where a central molecule of the crystal was selected and all its neighboring molecules were systematically identified. Atomic coordinates were measured with X-ray crystallography and obtained with the VESTA[62] and Avogadro programs.[63,64] Following our previous study,[21] the following model quantum chemistry was applied. Vertical excitation energies were computed with TD-DFT using the B3LYP density functional[65] and 6-31G(d′) basis set.[66,67] TD-DFT is the most practical method for calculating excited states in medium- and large-sized organic and inorganic molecules.[68,69] Moreover, this level of theory has produced qualitatively accurate linear and nonlinear absorption spectra of conjugated organic materials over a wide range of molecular sizes.[70–76] We validate the use of this model quantum chemistry, for the molecules of this paper, in Subsection III B.

In order to obtain OPA spectra, A, as a function of energy, Ω, each vertical excitation was given a Lorentzian lineshape

$$A_e(\Omega) \propto \frac{f_{ge}}{1 + 4\left(\frac{\Omega - \Omega_{ge}}{\Gamma}\right)^2}, \tag{2}$$

where f_{ge} is the oscillator strength between the ground and excited state, Ω_{ge} is the energy of the excited state, and Γ is the full width at half maximum (FWHM), which was set to a homogeneous broadening of 0.15 eV. The complete spectrum, A, is defined as the sum of all its individual contributions, A_e, i.e., $A = \sum_e A_e$. Here, 25 singlet excited states were requested in the TD-DFT calculation and used to compute each spectrum. Excited states were computed with the Gaussian 03 software package.[77] Since the most practical wavelength for initiation is in the NIR (near-infrared), we focus our attention to low-energy absorption peaks with relatively strong intensities. Therefore, spectra may be cut off at higher energies.

The two-photon absorption (TPA) of the monomers and dimers was computed using the extension of adiabatic TD-DFT to nonlinear optical response.[78,79] TPA spectra were also given Lorentzian lineshapes with FWHM of approximately 0.15 eV. It is worth noting that a rigorous choice of broadening was not of concern since the objective was to compare optical response between the monomers and dimers.

In order to determine the nature of the optical excitations in these chromophores, natural transition orbital (NTO) analysis was performed. NTOs offer a compact, qualitative representation of a transition density expanded in terms of single-particle transitions.[80,81] Therefore, NTOs provide a useful way of assigning transition character. Figures showing NTOs were obtained with the Jmol program.[82]

B. Benchmarking model quantum chemistry

To validate the proposed model quantum chemistry described in Subsection III A, theoretical ground-state geometries and optical absorption spectra were compared to experimental data. Monomers were optimized with no symmetry constraints using DFT and compared to those obtained from the experimental crystal structures. Maximum deviation of the bonds lengths between DFT and experiment was 0.015 Å. Experimental absorption spectra of these molecules dissolved in acetonitrile were obtained from our previous study,[21] and which are compared to the new TD-DFT calculations, shown in Fig. 2. Our previous calculations did not account for the effects of solvent on optical properties, but were rather, carried out in the gas phase. Here, we have calculated the absorption in solvent, as this makes for a better comparison to the available experimental data. Both non-equilibrium, linear response[83,84] (LR) and non-equilibrium state-specific[85,86]

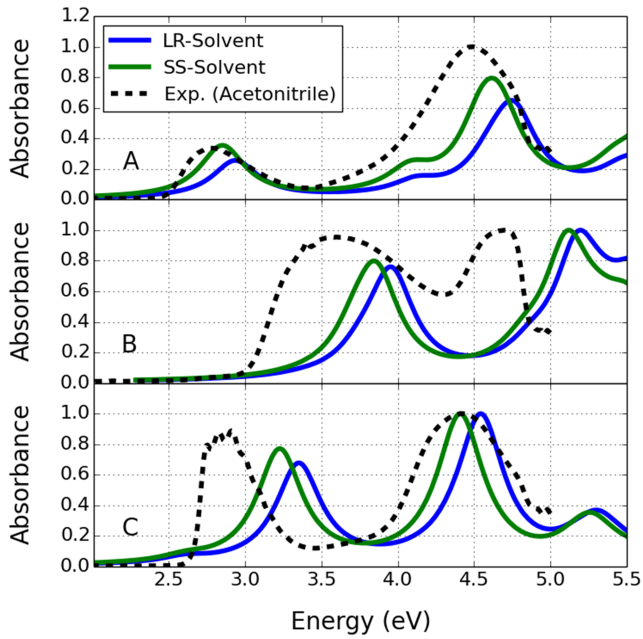

FIG. 2. Optical absorption of **A** through **C** in acetonitrile. Bold lines are theoretical spectra, determined using TD-DFT, while dashed lines are experimental. Experimental spectra were recorded with a HP 853 Agilent UV–Vis spectrometer. Materials were dissolved in solutions of acetonitrile at concentrations on the order of 10^{-4}M. Extinction coefficients were averaged over three solutions.

(SS) solvents were used with a polarizable continuum model (PCM).[87,88] The PCM models the solute as a system embedded in a dielectric cavity, with a dielectric constant ϵ that is characteristic of the solvent. In this case, acetonitrile has a dielectric constant of $\epsilon \approx 37.5$. The PCM is the most popular solvent model and has, for example, been successful in modeling solvated charge transfer states.[89] The theoretical OPA spectra in Fig. 2 were constructed using the method described in Subsection III A using a FWHM of 0.36 eV. This FWHM was chosen to closely match theory to experiment. A total of 50 singlet excited states were requested in the TD-DFT calculations and used to compute each spectrum. It is worth noting that we are in pursuit of predominantly qualitative models of OPA and TPA lineshapes. Therefore, theoretical spectra do not account for Franck-Condon effects or the changes in zero-point vibrational energies. That being said, excitation energies of vertical transitions have been found to be blue-shifted by about 0.2–0.3 eV relative to those of 0–0 transitions in rigid molecules.[90] In regards to error compensation due to choice of density functional, B3LYP with vibronic effects has proven to be in excellent quantitative agreement to experiment for large organic molecules.[90] All spectra of Fig. 2, experimental and theoretical, were normalized by maximum absorption to convey relative intensity. Optimized geometries and excited states were computed with the Gaussian 09 software package.[91]

In Fig. 2, TD-DFT matches the experimental spectrum of **A** exceptionally well, with a maximum deviation of 0.10 eV. The peaks in **B** and **C** are also recovered but with slightly larger blue-shifts. The relative intensities of all peaks in **A** through **C** are also accurately recovered. Therefore, although TD-DFT is generally more accurate for larger systems,[68,69] we expect this level of theory to be valuable for predicting the linear and nonlinear optical response in these smaller systems as well. It is worth reiterating that the geometries used to compute the spectra in Sec. IV were obtained from experimental crystal structures, as opposed to the optimized structures used in this subsection.

IV. RESULTS AND DISCUSSION

The OPA spectra of monomer **A** and its dimers are shown in the bottom panels of Fig. 3. OPA intensities of the dimers were halved in order to eliminate dependence on the number of

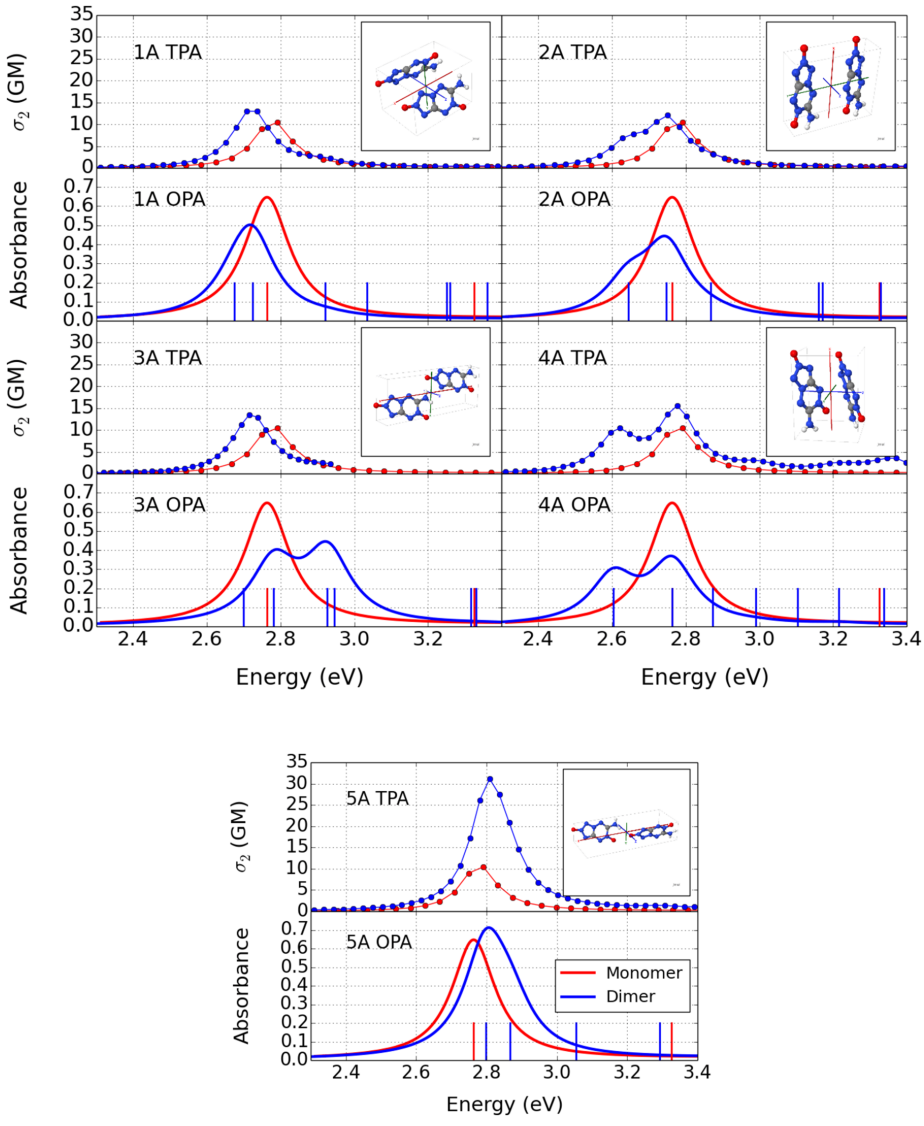

FIG. 3. OPA (bottom panel) and TPA (top panel) spectra of the monomer and dimers of material **A**. Results for the monomer are shown in red, while those of the dimers are shown in blue. Vertical lines in the bottom panels are vertical excitation energies determined from TD-DFT. OPA and TPA intensities of the dimers are halved, while the TPA energy scale is doubled to show total photon energy absorbed. Associated dimer configurations are shown.

chromophore units. Monomer **A** peaks at 2.76 eV, while dimers **1A** through **5A** peak between 2.72 and 2.92 eV. Compared to **A**, the OPA of **1A**, **2A**, and **4A** is shifted towards lower energy due to the optically active states at 2.68, 2.64, and 2.60 eV, respectively. The dimers also absorb with larger and more broadened intensities than the monomer. To account for changes in both peak intensity and broadening, the enhancement factor (EF) is defined as

$$\mathrm{EF} = \frac{1}{2}\frac{\int A_{\mathrm{Dim}}(\Omega)\,\mathrm{d}\Omega}{\int A_{\mathrm{Mon}}(\Omega)\,\mathrm{d}\Omega}, \tag{3}$$

where the integral is over the peak of interest, A is absorbance, and the factor of one-half removes the dependence on the number of chromophore units. EFs of **1A** through **5A** are between 0.6 and 1.1. For two non-interacting chromophore units, a 2-fold enhancement from monomer to dimer is expected since OPA depends on the transition dipole moments between the ground and excited states, which roughly scales linearly with the number of chromophore units, i.e., $|\mu_{ge}|^2 \propto N$. The data qualitatively agree with this reasoning. Overall, the dimers shift OPA by roughly 0.20 eV compared to that of the monomer.

The TPA spectra of monomer **A** and its dimers are shown in the top panels of Fig. 3. TPA intensities of the dimers were halved in order to eliminate the dependence on the number of chromophore units. Monomer **A** peaks in a similar location as its OPA state at 2.76 eV. TPA of **1A** through **5A** peak between 2.71 and 2.81 eV. The locations of OPA and TPA roughly coincide for all dimers, except for dimer **3A**, which has a dark OPA but bright TPA state at 2.70 eV. This state is red-shifted relative to the lowest-energy OPA state at 2.78 eV. This shows that TPA can be tuned to lower energies and activate dark OPA states. Such shifts are more pronounced in larger and more conjugated systems.[75] Similar to OPA of the dimers, there is also enhanced broadening in the TPA. The left shoulder in **2A** is due to the state at 2.64 eV, which is not optically active in **A**. The same is observed in **4A**, where the low-energy peak is located at 2.60 eV. Optically active low-energy TPA states are important, in practice, for initiation with conventional NIR lasers.

The most distinctive feature between the optical properties of the monomers and dimers is a cooperative enhancement in the TPA. Cooperative enhancement occurs when the TPA of a dimer is more than twice that of the monomer. Following the same definition for enhancement as OPA, $\mathrm{EF}_{\mathrm{TPA}}$s of **1A** through **5A** are 1.3, 1.5, 2.0, 2.4, and 3.0, respectively. The relatively large enhancement in **4A**, for example, can be attributed to the low-energy TPA state. Dimer **5A** is predicted to have the largest enhancement. Compared to the other dimers, **5A** is the largest in length, with two molecules nearly head-to-tail, as shown in Fig. 3, suggesting that this orientation induces a large enhancement in the TPA. We will later justify this within a two-level model.

A similar analysis can be made for the OPA and TPA spectra of materials **B** and **C**. For the sake of brevity, spectra with largest enhancements are shown in Fig. 4. OPA of monomer **B** peaks at 4.26 eV, while dimer **1B** has a broader band that is shifted towards lower energy and peaks at 3.96 eV. OPA of monomer **C** and dimer **1C** peaks in similar locations around 2.50 and 3.25 eV. The low-energy OPA peak is predicted to have a much lower intensity than the high-energy OPA peak in both **C** and **1C**. $\mathrm{EF}_{\mathrm{OPA}}$s of **1B** and the high-energy peak in **1C** are 1.0 and 1.1, respectively. TPA of **1B** is red-shifted relative to the TPA of **B**. There is also a TPA state in **1B** at 3.13 eV that is not optically active in **B**. Again, TPA of **C** and **1C** peaks in similar locations around 2.50 and 3.25 eV. Unlike OPA, however, the low-energy TPA peak is predicted to have a larger intensity than the high-energy TPA peak. $\mathrm{EF}_{\mathrm{TPA}}$ of **1B** and the low-energy peak of **1C** are estimated to be 3.5 and 5.6, respectively. Similar to **A**, multiple chromophore units strongly affect TPA in these materials. All data are summarized in Table II.

Within this small data set, there are several structure-property relationships. The first of which is the dependence of conjugation on TPA cross section, σ_2. Monomers **A** and **B** are more conjugated than **C** due to the tetrazine-tetrazolo and triazine-triazolo fused ring systems, respectively. The only conjugation in **C** is from the tetrazine ring. Therefore, the molecular orbitals of **A** and **B** are delocalized to a larger fraction of the molecule, which increases their transition dipole moments. Table II shows σ_2^{max} of **A** and **B** being 2 to 3 times larger than that of **C**.

A second structure-property relationship is the effect of orientation on cooperative enhancement. It is beneficial to elucidate the enhancement in a representative dimer with relatively large σ_2. The head-to-tail orientation of dimer **5A** results in an $\mathrm{EF}_{\mathrm{TPA}}$ of 3.0, which can be explained within the two-level model. When the ground and first couple excited states are well separated from higher-lying excited states, the sum over states expression for the second hyperpolarizability can be simplified. Furthermore, when the dipole moment is

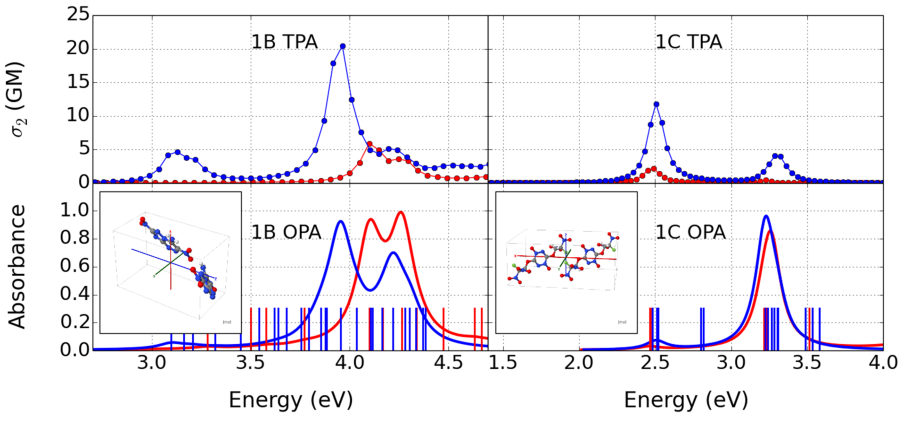

FIG. 4. OPA (bottom panel) and TPA (top panel) spectra of the monomer and dimers of materials **B** and **C**. Details of the spectra are the same as those described in Fig. 3.

TABLE II. Properties of OPA and TPA spectra in materials **A** through **C**. $\Omega_{OPA/TPA}$ are transition energies at maximum OPA and TPA, respectively. $EF_{OPA/TPA}$ are enhancement factors, as defined in Eq. (3). $EF^{max}_{OPA/TPA}$ are enhancements factors of peak absorptions. σ_2^{max} are maxima of the halved two-photon cross sections.

Structure	Ω_{OPA} (eV)	EF_{OPA}	EF^{max}_{OPA}	Ω_{TPA} (eV)	EF_{TPA}	σ_2^{max} (GM)	EF^{max}_{TPA}
A	2.76	1.0	1.0	2.79	1.0	10	1.0
1A	2.72	0.8	0.8	2.71	1.3	13	1.3
2A	2.74	0.9	0.7	2.75	1.5	12	1.2
3A	2.92	1.1	0.7	2.72	2.0	14	1.4
4A	2.76	0.9	0.6	2.78	2.4	16	1.6
5A	2.81	1.2	1.1	2.81	3.0	31	3.1
B	4.26	1.0	1.0	4.10	1.0	5.9	1.0
1B	3.96	1.0	0.9	3.96	3.5	20	3.5
C	2.47	1.0	1.0	2.49	1.0	2.2	1.0
1C	2.51	···	···	2.51	5.6	12	5.5
C	3.26	1.0	1.0	3.23	1.0	0.5	1.0
1C	3.23	1.1	1.1	3.29	···	4.0	···

predominantly along a single molecular axis, only one tensorial component of the second hyperpolarizability is needed to obtain σ_2. At maximum TPA, $\sigma_2^{max} \propto \mu_{ge}^2(\mu_{ee} - \mu_{gg})^2$.[75] For monomer **A**, μ_{ge}, μ_{gg}, and μ_{ee} are 3.6, 8.1, and 5.6 D, while for **5A**, they are 6.5, 17.6, and 14.3 D, respectively. The ratio of σ_2^{max} at 2.82 eV is $\sigma_2^{\mathbf{5A}}/\sigma_2^{\mathbf{A}} \approx 2.84$; a roughly 8% deviation from the full calculation of 3.1, shown in Table II. The largest contribution is from the transition dipole moment, μ_{ge}. Fig. 5(a) shows how **5A**'s orientation both rotates μ_{ge} towards the oxygen substituent and increases its magnitude.

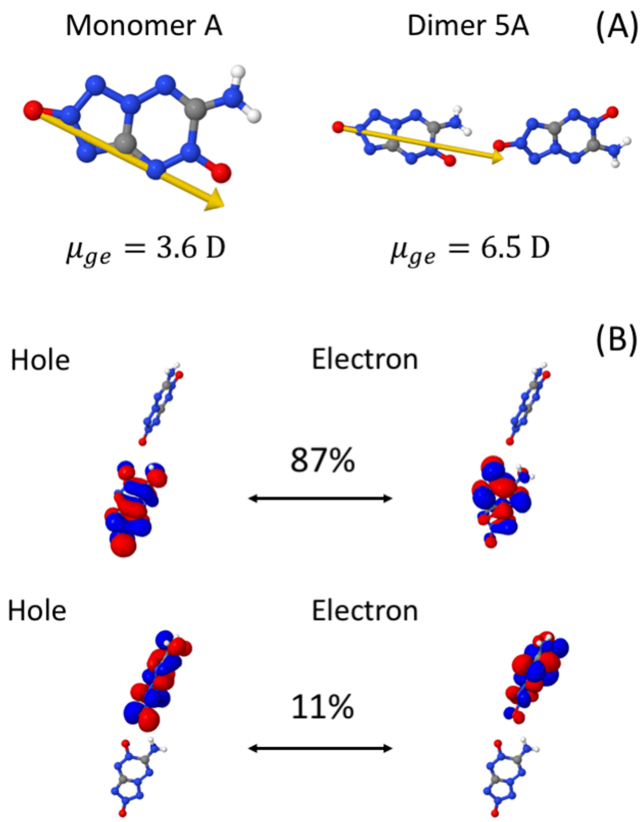

FIG. 5. (a) Magnitude and relative direction of μ_{ge} at 2.82 eV in monomer **A** and dimer **5A**. (b) NTOs of the vertical excitation in **5A**. Percentages are NTO eigenvalues.

The alternation of acceptor-donor substituents between the oxygen and NH_2 enhances electronic coupling. Moreover, the tetrazine-tetrazolo heterocycles enhance electronic delocalization over both chromophore units. Intermolecular coupling is evidenced by the $\pi-\pi^*$ transition shown in Fig. 5(b), where the excitation is on both chromophore units. A delocalized state due to optical excitation is common in conjugated systems.[92] Molecular packing in these explosive materials increases the degree of electronic delocalization, which inherently increases the nonlinear optical response, potentially making nonlinear laser initiation feasible.

V. CONCLUSIONS

We have utilized TD-DFT to model the OPA and TPA in energetic molecular materials that posses both enhanced safety and energetic performance properties compared to conventional energetic materials. The chosen level of theory was validated against experimental data. The geometries used to calculate the optical response of the monomers and dimers were extracted from their experimentally determined crystal structures. OPA scales linearly with the number of chromophore units, while TPA scales nonlinearly. Monomers **A** and **B** are more conjugated than **C** and have larger TPA cross sections. The most important feature of the optical response is a cooperative enhancement in the TPA of the dimers. Dimer **5A**, for example, showed a 6-fold enhancement in TPA peak intensity. Several dimers have two-photon active states at low energy, which is important for optical initiation with conventional NIR lasers. We predict that materials **A** and **C** can be excited via OPA and TPA with widely available double frequency (532 nm) and regular (1064 nm) Nd:YAG lasers, respectively. Overall, material **A** is predicted to have the optical range, intensity, and enhancement that are favorable for application.

This study has focused on isolated dimers, but even at this level, TPA is enhanced within the optical window of interest. A nonlinear increase in the TPA cross section is expected for these materials in bulk. Moreover, based on the results of Fig. 2, theoretical spectra are generally blue-shifted relative to experimental spectra. Therefore, predicted energies

may be overestimated, bringing the true window for optical excitation closer to the NIR. Due to the nature of cooperative enhancement in the nonlinear optical response, it is worth exploring more extended and conjugated structures for explosive applications. This work is part of an extended project to predict, design, and assess the applicability of novel photoactive energetic materials. Future work with these materials will entail nonadiabatic dynamics to determine photoproducts and relative time scales of decomposition.

ACKNOWLEDGMENTS

The authors acknowledge support of the U.S. Department of Energy through the Los Alamos National Laboratory (LANL) LDRD Program. LANL is operated by Los Alamos National Security, LLC, for the National Nuclear Security Administration of the U.S. Department of Energy under Contract No. DE-AC52- 06NA25396. This work was done in part at the Center for Nonlinear Studies (CNLS) and the Center for Integrated Nanotechnologies (CINT) at LANL. We also acknowledge the LANL Institutional Computing (IC) program for providing computational resources. O.V.P. and A.E.S. acknowledge support of the US Department of Energy, Grant No. DE-SC0014429. A.E.S. thanks CNLS for their hospitality.

[1] C. Bian, X. Dong, X. Zhang, Z. Zhou, M. Zhang, and C. Li, J. Mater. Chem. A **3**, 3594 (2015).
[2] Y. Tang, J. Zhang, L. A. Mitchell, D. A. Parrish, and J. M. Shreeve, J. Am. Chem. Soc. **137**, 15984 (2015).
[3] P. Yin and J. M. Shreeve, Angew. Chem., Int. Ed. **54**, 14513 (2015).
[4] P. Yin and J. M. Shreeve, Angew. Chem. **127**, 14721 (2015).
[5] D. E. Chavez, J. C. Bottaro, M. Petrie, and D. A. Parrish, Angew. Chem., Int. Ed. **54**, 12973 (2015).
[6] D. E. Chavez, J. C. Bottaro, M. Petrie, and D. A. Parrish, Angew. Chem. **127**, 13165 (2015).
[7] T. M. Klapötke, M. Leroux, P. C. Schmid, and J. Stierstorfer, Chem. - Asian J. **11**, 844 (2016).
[8] T. M. Klapötke, P. C. Schmid, S. Schnell, and J. Stierstorfer, Chem. - Eur. J. **21**, 9219 (2015).
[9] W. Fickett and W. C. Davis, *Detonation: Theory and Experiment* (Courier Corporation, 2012).
[10] E. Aluker, A. Krechetov, A. Y. Mitrofanov, and D. Nurmukhametov, Russ. J. Phys. Chem. B **5**, 658 (2011).
[11] D. Fischer, T. M. Klapötke, D. G. Piercey, and J. Stierstorfer, J. Energ. Mater. **30**, 40 (2012).
[12] N. Fischer, M. Joas, T. M. Klapötke, and J. Stierstorfer, Inorg. Chem. **52**, 13791 (2013).
[13] M. Joas, T. M. Klapötke, J. Stierstorfer, and N. Szimhardt, Chem. - Eur. J. **19**, 9995 (2013).
[14] J. Evers, I. Gospodinov, M. Joas, T. M. Klapötke, and J. Stierstorfer, Inorg. Chem. **53**, 11749 (2014).
[15] M. Joas, T. M. Klapötke, and N. Szimhardt, Eur. J. Inorg. Chem. **2014**, 493.
[16] M. T. Greenfield, S. D. McGrane, C. A. Bolme, J. A. Bjorgaard, T. R. Nelson, S. Tretiak, and R. J. Scharff, J. Phys. Chem. A **119**, 4846 (2015).
[17] T. Nelson, J. Bjorgaard, M. Greenfield, C. Bolme, K. Brown, S. McGrane, R. J. Scharff, and S. Tretiak, J. Phys. Chem. A **120**, 519 (2016).
[18] T. W. Myers, D. E. Chavez, S. K. Hanson, R. J. Scharff, B. L. Scott, J. M. Veauthier, and R. Wu, Inorg. Chem. **54**, 8077 (2015).
[19] T. W. Myers, J. A. Bjorgaard, K. E. Brown, D. E. Chavez, S. K. Hanson, R. J. Scharff, S. Tretiak, and J. M. Veauthier, J. Am. Chem. Soc. **138**, 4685 (2016).
[20] S. D. McGrane, C. A. Bolme, M. T. Greenfield, D. E. Chavez, S. K. Hanson, and R. J. Scharff, J. Phys. Chem. A **120**, 895 (2016).
[21] J. A. Bjorgaard, A. E. Sifain, T. R. Nelson, T. W. Myers, J. M. Veauthier, D. E. Chavez, R. J. Scharff, and S. Tretiak, J. Phys. Chem. A **120**, 4455 (2016).
[22] V. V. Chaban, S. Pal, and O. V. Prezhdo, J. Am. Chem. Soc. **138**, 15927 (2016).
[23] A. E. Sifain, J. A. Bjorgaard, T. W. Myers, J. M. Veauthier, D. E. Chavez, O. V. Prezhdo, R. J. Scharff, and S. Tretiak, J. Phys. Chem. C **120**, 28762 (2016).
[24] D. E. Chavez and M. A. Hiskey, J. Energ. Mater. **17**, 357 (1999).
[25] D. E. Chavez, M. A. Hiskey, and R. D. Gilardi, Angew. Chem. **112**, 1861 (2000).
[26] L. E. Fried, M. R. Manaa, P. F. Pagoria, and R. L. Simpson, Annu. Rev. Mater. Res. **31**, 291 (2001).
[27] P. F. Pagoria, G. S. Lee, A. R. Mitchell, and R. D. Schmidt, Thermochim. Acta **384**, 187 (2002).
[28] V. Thottempudi, F. Forohor, D. A. Parrish, and J. M. Shreeve, Angew. Chem., Int. Ed. **51**, 9881 (2012).
[29] H. Wei, J. Zhang, and J. M. Shreeve, Chem. - Asian J. **10**, 1130 (2015).
[30] P. Yin, Q. Zhang, and J. M. Shreeve, Acc. Chem. Res. **49**, 4 (2015).
[31] M. Schulze, B. Scott, and D. Chavez, J. Mater. Chem. A **3**, 17963 (2015).
[32] J. J. Sabatini and K. D. Oyler, Crystals **6**, 5 (2015).
[33] Y. Li, Y. Shu, B. Wang, S. Zhang, and L. Zhai, RSC Adv. **6**, 84760 (2016).
[34] P. W. Cooper, *Explosives Engineering* (Wiley-VCH, New York, 1996).
[35] D. E. Chavez, D. A. Parrish, L. Mitchell, and G. H. Imler, Angew. Chem., Int. Ed. **56**, 3575 (2017).
[36] D. E. Chavez, D. A. Parrish, L. Mitchell, and G. H. Imler, Angew. Chem. **129**, 3629 (2017).
[37] D. G. Piercey, D. E. Chavez, B. L. Scott, G. H. Imler, and D. A. Parrish, Angew. Chem., Int. Ed. **55**, 15315 (2016).
[38] D. G. Piercey, D. E. Chavez, B. L. Scott, G. H. Imler, and D. A. Parrish, Angew. Chem. **128**, 15541 (2016).
[39] D. E. Chavez, D. A. Parrish, and L. Mitchell, Angew. Chem., Int. Ed. **55**, 8666 (2016).
[40] D. E. Chavez, D. A. Parrish, and L. Mitchell, Angew. Chem. **128**, 8808 (2016).
[41] M. Drobizhev, A. Karotki, Y. Dzenis, A. Rebane, Z. Suo, and C. W. Spangler, J. Phys. Chem. B **107**, 7540 (2003).
[42] S.-J. Chung, K.-S. Kim, T.-C. Lin, G. S. He, J. Swiatkiewicz, and P. N. Prasad, J. Phys. Chem. B **103**, 10741 (1999).
[43] Y. Wang, G. S. He, P. N. Prasad, and T. Goodson, J. Am. Chem. Soc. **127**, 10128 (2005).
[44] M. Drobizhev, A. Karotki, A. Rebane, and C. W. Spangler, Opt. Lett. **26**, 1081 (2001).
[45] O. Varnavski, X. Yan, O. Mongin, M. Blanchard-Desce, and T. Goodson, J. Phys. Chem. C **111**, 149 (2007).
[46] M. Drobizhev, A. Karotki, M. Kruk, and A. Rebane, Chem. Phys. Lett. **355**, 175 (2002).
[47] M. Drobizhev, Y. Stepanenko, Y. Dzenis, A. Karotki, A. Rebane, P. N. Taylor, and H. L. Anderson, J. Am. Chem. Soc. **126**, 15352 (2004).
[48] M. Drobizhev, Y. Stepanenko, Y. Dzenis, A. Karotki, A. Rebane, P. N. Taylor, and H. L. Anderson, J. Phys. Chem. B **109**, 7223 (2005).
[49] M. Drobizhev, Y. Stepanenko, A. Rebane, C. J. Wilson, T. E. Screen, and H. L. Anderson, J. Am. Chem. Soc. **128**, 12432 (2006).
[50] H. Ceymann, A. Rosspeintner, M. H. Schreck, C. Mützel, A. Stoy, E. Vauthey, and C. Lambert, Phys. Chem. Chem. Phys. **18**, 16404 (2016).
[51] F. Terenziani, V. Parthasarathy, A. Pla-Quintana, T. Maishal, A.-M. Caminade, J.-P. Majoral, and M. Blanchard-Desce, Angew. Chem., Int. Ed. **48**, 8691 (2009).
[52] A. Mikhaylov, D. V. Kondratuk, A. Cnossen, H. L. Anderson, M. Drobizhev, and A. Rebane, J. Phys. Chem. C **120**, 11663 (2016).
[53] T. W. Myers, C. J. Snyder, D. E. Chavez, R. J. Scharff, and J. M. Veauthier, Chem. - Eur. J. **22**, 10590 (2016).
[54] C. He and J. M. Shreeve, Angew. Chem., Int. Ed. **54**, 6260 (2015).
[55] C. He and J. M. Shreeve, Angew. Chem. **127**, 6358 (2015).
[56] L. Fried, W. Howard, S. Bastea, K. Glaesmann, P. Souers, P. Vitello, and I. Kuo, *CHEETAH Thermochemical Code* (Lawrence Livermore National Laboratory, Livermore, CA, USA, 2007).
[57] E. F. Byrd and B. M. Rice, J. Phys. Chem. A **110**, 1005 (2006).
[58] E. F. Byrd and B. M. Rice, J. Phys. Chem. A **113**, 5813 (2009).
[59] M. A. Kettner, T. M. Klapötke, T. G. Witkowski, and F. von Hundling, Chem. - Eur. J. **21**, 4238 (2015).
[60] Q. J. Axthammer, B. Krumm, and T. M. Klapötke, J. Org. Chem. **80**, 6329 (2015).
[61] J. P. Agrawal, *High Energy Materials*, Propellants, Explosives and Pyrotechnics (Wiley-VCH, Weinheim, Germany, 2010).
[62] K. Momma and F. Izumi, J. Appl. Crystallogr. **44**, 1272 (2011).
[63] Avogadro: An Open-Source Molecular Builder and Visualization Tool. Version 1.1.1, accessed 1 September, 2016, http://avogadro.openmolecules.net/.

[64]M. D. Hanwell, D. E. Curtis, D. C. Lonie, T. Vandermeersch, E. Zurek, and G. R. Hutchison, J. Cheminf. **4**, 1 (2012).
[65]A. D. Becke, J. Chem. Phys. **98**, 5648 (1993).
[66]A. Petersson, A. Bennett, T. G. Tensfeldt, M. A. Al-Laham, W. A. Shirley, and J. Mantzaris, J. Chem. Phys. **89**, 2193 (1988).
[67]G. Petersson and M. A. Al-Laham, J. Chem. Phys. **94**, 6081 (1991).
[68]D. Jacquemin, V. Wathelet, E. A. Perpete, and C. Adamo, J. Chem. Theory Comput. **5**, 2420 (2009).
[69]A. Dreuw and M. Head-Gordon, Chem. Rev. **105**, 4009 (2005).
[70]A. Masunov and S. Tretiak, J. Phys. Chem. B **108**, 899 (2004).
[71]E. A. Badaeva, T. V. Timofeeva, A. Masunov, and S. Tretiak, J. Phys. Chem. A **109**, 7276 (2005).
[72]C. Katan, F. Terenziani, O. Mongin, M. H. Werts, L. Porres, T. Pons, J. Mertz, S. Tretiak, and M. Blanchard-Desce, J. Phys. Chem. A **109**, 3024 (2005).
[73]J. F. Kauffman, J. M. Turner, I. V. Alabugin, B. Breiner, S. V. Kovalenko, E. A. Badaeva, A. Masunov, and S. Tretiak, J. Phys. Chem. A **110**, 241 (2006).
[74]E. Badaeva and S. Tretiak, Chem. Phys. Lett. **450**, 322 (2008).
[75]F. Terenziani, C. Katan, E. Badaeva, S. Tretiak, and M. Blanchard-Desce, Adv. Mater. **20**, 4641 (2008).
[76]C. Katan, M. Charlot, O. Mongin, C. Le Droumaguet, V. Jouikov, F. Terenziani, E. Badaeva, S. Tretiak, and M. Blanchard-Desce, J. Phys. Chem. B **114**, 3152 (2010).
[77]M. J. Frisch, G. W. Trucks, H. B. Schlegel, G. E. Scuseria, M. A. Robb, J. R. Cheeseman, G. Scalmani, V. Barone, B. Mennucci, G. A. Petersson, H. Nakatsuji, M. Caricato, X. Li, H. P. Hratchian, A. F. Izmaylov, J. Bloino, G. Zheng, J. L. Sonnenberg, M. Hada, M. Ehara, K. Toyota, R. Fukuda, J. Hasegawa, M. Ishida, T. Nakajima, Y. Honda, O. Kitao, H. Nakai, T. Vreven, J. A. Montgomery, Jr., J. E. Peralta, F. Ogliaro, M. Bearpark, J. J. Heyd, E. Brothers, K. N. Kudin, V. N. Staroverov, R. Kobayashi, J. Normand, K. Raghavachari, A. Rendell, J. C. Burant, S. S. Iyengar, J. Tomasi, M. Cossi, N. Rega, J. M. Millam, M. Klene, J. E. Knox, J. B. Cross, V. Bakken, C. Adamo, J. Jaramillo, R. Gomperts, R. E. Stratmann, O. Yazyev, A. J. Austin, R. Cammi, C. Pomelli, J. W. Ochterski, R. L. Martin, K. Morokuma, V. G. Zakrzewski, G. A. Voth, P. Salvador, J. J. Dannenberg, S. Dapprich, A. D. Daniels, Ö. Farkas, J. B. Foresman, J. V. Ortiz, J. Cioslowski, and D. J. Fox, GAUSSIAN 03, Revision E. 01, Gaussian, Inc., 2004.
[78]O. Berman and S. Mukamel, Phys. Rev. A **67**, 042503 (2003).
[79]S. Tretiak and V. Chernyak, J. Chem. Phys. **119**, 8809 (2003).
[80]R. L. Martin, J. Chem. Phys. **118**, 4775 (2003).
[81]E. R. Batista and R. L. Martin, *Encyclopedia of Computational Chemistry* (Wiley Online Library, Hoboken, NJ, 2004).
[82] Jmol: An Open-Source Java Viewer for Chemical Structures in 3D, accessed 1 September, 2016, http://www.jmol.org/.
[83]R. Cammi, B. Mennucci, and J. Tomasi, J. Phys. Chem. A **104**, 5631 (2000).
[84]M. Cossi and V. Barone, J. Chem. Phys. **115**, 4708 (2001).
[85]R. Improta, V. Barone, G. Scalmani, and M. J. Frisch, J. Chem. Phys. **125**, 054103 (2006).
[86]R. Improta, G. Scalmani, M. J. Frisch, and V. Barone, J. Chem. Phys. **127**, 074504 (2007).
[87]G. Scalmani, M. J. Frisch, B. Mennucci, J. Tomasi, R. Cammi, and V. Barone, J. Chem. Phys. **124**, 094107 (2006).
[88]B. Mennucci, Wiley Interdiscip. Rev.: Comput. Mol. Sci. **2**, 386 (2012).
[89]S. Zheng, E. Geva, and B. D. Dunietz, J. Chem. Theory Comput. **9**, 1125 (2013).
[90]M. Dierksen and S. Grimme, J. Chem. Phys. **120**, 3544 (2004).
[91]M. J. Frisch, G. W. Trucks, H. B. Schlegel, G. E. Scuseria, M. A. Robb, J. R. Cheeseman, G. Scalmani, V. Barone, B. Mennucci, G. A. Petersson, H. Nakatsuji, M. Caricato, X. Li, H. P. Hratchian, A. F. Izmaylov, J. Bloino, G. Zheng, J. L. Sonnenberg, M. Hada, M. Ehara, K. Toyota, R. Fukuda, J. Hasegawa, M. Ishida, T. Nakajima, Y. Honda, O. Kitao, H. Nakai, T. Vreven, J. A. Montgomery, Jr., J. E. Peralta, F. Ogliaro, M. Bearpark, J. J. Heyd, E. Brothers, K. N. Kudin, V. N. Staroverov, R. Kobayashi, J. Normand, K. Raghavachari, A. Rendell, J. C. Burant, S. S. Iyengar, J. Tomasi, M. Cossi, N. Rega, J. M. Millam, M. Klene, J. E. Knox, J. B. Cross, V. Bakken, C. Adamo, J. Jaramillo, R. Gomperts, R. E. Stratmann, O. Yazyev, A. J. Austin, R. Cammi, C. Pomelli, J. W. Ochterski, R. L. Martin, K. Morokuma, V. G. Zakrzewski, G. A. Voth, P. Salvador, J. J. Dannenberg, S. Dapprich, A. D. Daniels, Ö. Farkas, J. B. Foresman, J. V. Ortiz, J. Cioslowski, and D. J. Fox, GAUSSIAN 09, Revision D. 02, Gaussian, Inc., 2009.
[92]M. I. Ranasinghe, O. P. Varnavski, J. Pawlas, S. I. Hauck, J. Louie, J. F. Hartwig, and T. Goodson, J. Am. Chem. Soc. **124**, 6520 (2002).